Dalton Transactions

Cite this: *Dalton Trans.*, 2011, **40**, 9276

www.rsc.org/dalton

PAPER

The co-ordination chemistry of tris(3,5-dimethylpyrazolyl)methane manganese carbonyl complexes: Synthetic, electrochemical and DFT studies†

Andrew J. Hallett,*[a] R. Angharad Baber,[b] A. Guy Orpen[b] and Benjamin D. Ward[a]

Received 3rd May 2011, Accepted 24th June 2011
DOI: 10.1039/c1dt10828j

The tricarbonyl $[Mn(CO)_3\{HC(pz')_3\}][PF_6]$ $\mathbf{1}^+[PF_6]^-$ (pz′ = 3,5-dimethylpyrazolyl) reacts with a range of *P*-, *N*- and *C*-donor ligands, L, in the presence of trimethylamine oxide to give $[Mn(CO)_2L\{HC(pz')_3\}]^+$ {L = PEt_3 $\mathbf{3}^+$, $P(OEt)_3$ $\mathbf{4}^+$, $P(OCH_2)_3CEt$ $\mathbf{5}^+$, py $\mathbf{6}^+$, MeCN $\mathbf{7}^+$, $CNBu^t$ $\mathbf{8}^+$ and CNXyl $\mathbf{9}^+$}. The complex $[Mn(CO)_2(PMe_3)\{HC(pz')_3\}]^+$ $\mathbf{2}^+$ is formed by reaction of $\mathbf{7}^+$ with PMe_3. Complexes $\mathbf{2}^+$ and $\mathbf{6}^+$ were structurally characterised by X-ray diffraction methods. Reaction of $\mathbf{7}^+$ with half a molar equivalent of 4,4′-bipyridine gives a purple compound assumed to be the bridged dimer $[\{HC(pz')_3\}Mn(CO)_2(\mu\text{-}4,4'\text{-bipy})Mn(CO)_2\{HC(pz')_3\}]^{2+}$ $\mathbf{10}^{2+}$. The relative electron donating ability of $HC(pz')_3$ has been established by comparison with the cyclopentadienyl and tris(pyrazolyl)borate analogues. Cyclic voltammetry shows that each of the complexes undergoes an irreversible oxidation. The correlation between the average carbonyl stretching frequency and the oxidation potential for complexes of *P*- and *C*-donor ligands is coincident with the correlation observed for $[Mn(CO)_{3-m}L_m(\eta\text{-}C_5H_{5-n}Me_n)]$. The data for complexes of *N*-donor ligands, however, are not coincident due to the presence of a node (and phase change) between the metal and the *N*-donor in the HOMO of the complex as suggested by preliminary DFT calculations.

Introduction

Poly(pyrazolyl)alkane ligands of the type $R_{4-n}C(pz^x)_n$ ($n = 2$, 3 or 4) are neutral analogues of poly(pyrazolyl)borate anions (Fig. 1).[1,2] The $HC(pz')_3$ ligand is considerably less basic than anionic Tp^- or Cp^- and may also be considered analogous to C_6H_6 as they are both neutral, facially-capping, six-electron donors.

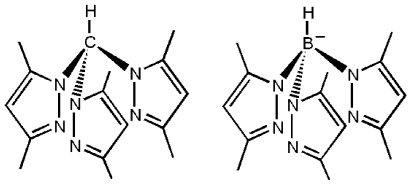

Fig. 1 Neutral tris(3,5-dimethylpyrazolyl)methane $[HC(pz')_3]$ and anionic hydrotris(3,5-dimethylpyrazolyl)borate, Tp′, ligands.

Poly(pyrazolyl)borate anions $[R_{4-n}B(pz)_n]^-$ (n = 2, 3 or 4) have commonly been used in co-ordination chemistry as their steric and electronic properties are easily modified by changing the number of, and substituents on, the pyrazolyl rings and the substituents, R, at the boron centre.[3–5] Tris(pyrazolyl)methane ligands are not as comprehensively studied as their tris(pyrazolyl)borate analogues due to the relative difficulty of preparation. However, in recent years complexes of poly(pyrazolyl)alkane ligands have become more documented[6,7] partly due to an improved synthesis by Reger *et al.*[8]

Manganese tricarbonyl complexes have been studied for their CO-releasing properties in photosubstitution reactions.[9,10] These CORMs (CO-Releasing Molecules) release CO upon UV irradiation and exhibit cytotoxic activity against cancer cells.[11,12] Substitution of the carbonyls in the manganese complexes with various ligands gives mono and dicarbonyl species. Indeed, the cyclopentadienyl complexes $[Mn(CO)_3Cp^*]$ and $[Mn(CO)_3Cp]$ and the tetrakis(pyrazolyl)borate complex $[Mn(CO)_3\{(pz)B(pz)_3\}]$ undergo photochemical substitution reactions with a range of nucleophilic ligands.[13–15] However, the degree of substitution depends on the size of the ligand L. An increase in the steric requirements of the pyrazolyl group by the presence of methyl substituents in $[Mn(CO)_3Tp']$ leads to mono-substitution only with $P(OMe)_3$, $P(OPh)_3$ and PMe_3 (*i.e.* only those ligands with small cone angles). Substitution of carbonyls was also reported in the [11]ane-P_2C^{NHC} macrocyclic tricarbonyl complexes of Re and Mn using Me_3NO.[16,17]

Manganese tricarbonyl complexes of several functionalised poly(pyrazolyl)alkanes such as tris(pyrazolyl)methane,[8,18] multitopic ligands,[19] and [di(pyrazolyl)(2-pyridyl)methyl]aryl

[a]*School of Chemistry, Cardiff University, Main Building, Park Place, Cardiff, CF10 3AT, UK. E-mail: hallettaj@cardiff.ac.uk; Fax: +44 029 20874030; Tel: +44 029 20879316*
[b]*School of Chemistry, University of Bristol, Cantock's Close, Bristol, BS8 1TS, UK*

† CCDC reference numbers 822692–822693. For crystallographic data in CIF or other electronic format see DOI: 10.1039/c1dt10828j

scorpionates[13,20] have been reported. However, unlike for the cyclopentadienyl[15] and poly(pyrazolyl) complexes,[14,21] there is no literature reporting the substitution of CO.

Here we describe the synthesis of a range of manganese complexes $[Mn(CO)_2L\{HC(pz')_3\}]^+$ {L = CO, PMe_3, PEt_3, $P(OEt)_3$, $P(OCH_2)_3CEt$, py, MeCN, CN*t*Bu, CNXyl} in which the pyrazolylmethane ligand occupies three co-ordination sites around the octahedral manganese metal centre. Manganese dicarbonyl complexes were chosen as they are readily obtainable, CO vibrations can easily be monitored by IR spectroscopy and are oxidised more readily than the analogous tricarbonyl complexes.

Results and discussion

Synthesis and characterisation of tris(3,5-dimethylpyrazolyl)methane manganese complexes

The manganese tricarbonyl complex $[Mn(CO)_3\{HC(pz')_3\}][PF_6]$ $\mathbf{1}^+[PF_6]^-$ was prepared in two stages, by reacting $[MnBr(CO)_5]$ with tris(3,5-dimethylpyrazolyl)methane and subsequent addition of ammonium hexafluorophosphate. UV irradiation in the presence of various coordinating ligands (phosphines, *etc.*) did not give the desired mono- or di-substituted manganese products, but led to complete decomposition. However, the neutral tris(pyrazolyl)methane ligand makes complexes such as $[Mn(CO)_3\{HC(pz')_3\}]^+$ $\mathbf{1}^+$ more susceptible to nucleophilic attack at CO than analogous pyrazolylborate complexes. Thus, complex $\mathbf{1}^+$ does react with various ligands in the presence of trimethylamine oxide to give monosubstituted dicarbonyls (Scheme 1). As with the pyrazolylborate analogue,[21] there was no reaction between $[Mn(CO)_3\{HC(pz')_3\}]^+$ and PPh_3 or PCy_3 (*i.e.* phosphines with larger cone angles).

An alternative route to complexes $\mathbf{2}^+$–$\mathbf{6}^+$ and $\mathbf{8}^+$–$\mathbf{9}^+$ involved the reaction of $[Mn(CO)_2(NCMe)\{HC(pz')_3\}]^+$ $\mathbf{7}^+$ with L in CH_2Cl_2. Indeed, the synthesis of $\mathbf{2}^+$ can only be accomplished by this route. Reaction of $\mathbf{1}^+$ with Me_3NO in the presence of PMe_3 does not result in substitution, only oxidation of the phosphine. In addition, the reaction of $\mathbf{7}^+$ with half a molar equivalent of 4,4′-bipyridine in CH_2Cl_2 yields a moderately soluble purple complex, $\mathbf{10}^{2+}$, showing two IR carbonyl stretching bands and is assumed to be $[\{HC(pz')_3\}(CO)_2Mn(\mu\text{-}4,4'\text{-bipy})Mn(CO)_2\{HC(pz')_3\}][PF_6]_2$ (Fig. 2). Dissolving $\mathbf{10}^{2+}$ in acetonitrile results in a purple to yellow colour change (over *ca.* ten minutes) and an IR carbonyl stretching frequency identical to that of $[Mn(CO)_2(NCMe)\{HC(pz')_3\}]^+$ $\mathbf{7}^+$.

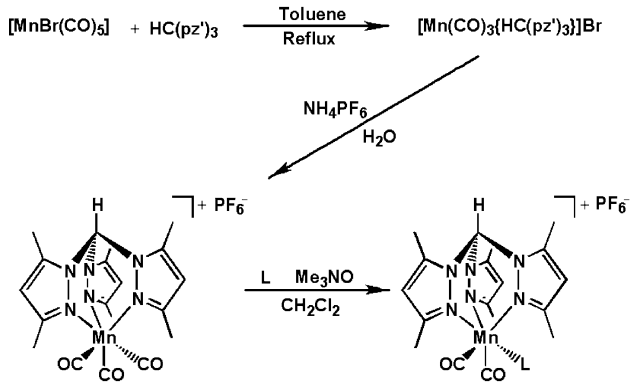

Scheme 1 Synthetic route to $[Mn(CO)_2L\{HC(pz')_3\}][PF_6]$.

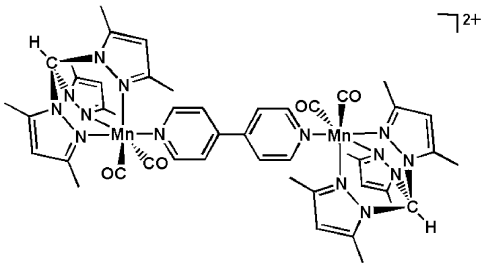

Fig. 2 The proposed structure of $\mathbf{10}^{2+}$.

Surprisingly, there was no reaction between $\mathbf{7}^+$ and 2,2′-bipyridine, even in refluxing $CHCl_3$, possibly due to increased steric interactions. Indeed, for the substitution reactions of $\mathbf{1}^+$ only one carbonyl ligand was substituted in all cases, affording the complexes $\mathbf{3}^+$–$\mathbf{10}^+$. Both the cyclopentadienyl[15] and pyrazolylborate[14,21] analogues give mono- and di-substituted complexes. In addition, the use of bidentate ligands such as dppe {1,2-bis(diphenylphosphino)ethane} did not induce substitution. This is perhaps not so surprising given that there was also no reaction with PPh_3.

Complexes $\mathbf{1}^+$–$\mathbf{10}^{2+}$ were characterised by elemental analysis (Table 1), X-ray crystallography in the cases of $\mathbf{2}^+$ and $\mathbf{6}^+$, ^1H NMR spectroscopy (except for $\mathbf{10}^{2+}$), IR spectroscopy (Table 1) and cyclic voltammetry (Table 5).

Table 1 Analytical and IR spectroscopic data for $[Mn(CO)_2L\{HC(pz')_3\}]^+$ and $[\{HC(pz')_3\}(CO)_2Mn(\mu\text{-}4,4'\text{-bipy})Mn(CO)_2\{HC(pz')_3\}]^{2+}$

		Analysis (%)[b]			IR[c]/cm^{-1}	
Complex[a]	Colour	C	H	N	*ν*(CO)	*ν*(CN)
$[Mn(CO)_3\{HC(pz')_3\}]^+$ $\mathbf{1}^+$	yellow	39.4 (39.2)	3.7 (3.8)	14.3 (14.4)	2045, 1950(b)	—
$[Mn(CO)_2(PMe_3)\{HC(pz')_3\}]^+$ $\mathbf{2}^+$	yellow	36.6 (36.6)	5.0 (4.7)	11.9 (11.8)[d]	1945, 1866	—
$[Mn(CO)_2(PEt_3)\{HC(pz')_3\}]^+$ $\mathbf{3}^+$	yellow	40.9 (41.2)	5.3 (5.4)	12.0 (11.8)[e]	1942, 1864	—
$[Mn(CO)_2\{P(OEt_3)\}\{HC(pz')_3\}]^+$ $\mathbf{4}^+$	yellow	35.3 (35.1)	4.6 (4.6)	9.7 (9.4)[f]	1963, 1886	—
$[Mn(CO)_2\{P(OCH_2)_3CEt\}\{HC(pz')_3\}]^+$ $\mathbf{5}^+$	yellow	35.2 (35.2)	4.2 (4.2)	9.6 (9.5)[f]	1976, 1900	—
$[Mn(CO)_2(py)\{HC(pz')_3\}]^+$ $\mathbf{6}^+$	orange	42.1 (41.8)	4.2 (4.2)	14.7 (14.5)[e]	1945, 1861	—
$[Mn(CO)_2(MeCN)\{HC(pz')_3\}]^+$ $\mathbf{7}^+$	orange	38.4 (38.6)	4.2 (4.1)	15.2 (15.4)[e]	1960, 1877	—
$[Mn(CO)_2(CNBu^t)\{HC(pz')_3\}]^+$ $\mathbf{8}^+$	yellow	41.6 (41.5)	4.7 (4.7)	14.2 (14.4)[e]	1963, 1896	2136
$[Mn(CO)_2(CNXyl)\{HC(pz')_3\}]^+$ $\mathbf{9}^+$	yellow	45.2 (45.4)	4.0 (4.4)	13.2 (13.5)[e]	1964, 1907	2106
$[\{HC(pz')_3\}(CO)_2Mn(\mu\text{-}4,4'\text{-bipy})Mn(CO)_2\{HC(pz')_3\}]^{2+}$ $\mathbf{10}^{2+}$	purple	41.5 (41.8)	4.3 (4.0)	14.4 (14.5)[d]	1946, 1865	—

[a] Isolated as $[PF_6]^-$ salts. [b] Calculated values in parentheses. [c] Recorded as CH_2Cl_2 solutions. [d] Analysed as a 1 : 1 CH_2Cl_2 solvate. [e] Analysed as a 2 : 1 CH_2Cl_2 solvate. [f] Analysed as a 1 : 2 CH_2Cl_2 solvate.

Table 2 Carbonyl stretching frequencies of $[Mn(CO)_3(Ligand)]$ (Ligand = Cp*, Cp, Tp′ and Tp) and $[Mn(CO)_3\{HC(pz')_3\}][PF_6]$ $\mathbf{1}^+[PF_6]^-$

Ligand	ν(CO)/cm^{-1}
Cp*	2017, 1929[28]
Cp	2028, 1947[26]
Tp′	2032, 1927[21]
Tp	2042, 1941[21]
$HC(pz')_3$	2045, 1950

Table 3 Selected bond lengths (Å) and angles (°) for $[Mn(CO)_2(PMe_3)\{HC(pz')_3\}][PF_6]$ $\mathbf{2}^+[PF_6]^-$ and $[Mn(CO)_2(py)\{HC(pz')_3\}][PF_6]\cdot 2CH_2Cl_2$ $\mathbf{6}^+[PF_6]^-\cdot 2CH_2Cl_2$

Bond length (Å)/angle (°)	$\mathbf{2}^+[PF_6]^-$	$\mathbf{6}^+[PF_6]^-\cdot 2CH_2Cl_2$
Mn(1)–C(1)	1.755(8)	1.774(6)
Mn(1)–C(2)	1.756(8)	1.757(6)
Mn(1)–N(1)	2.064(5)	2.052(4)
Mn(1)–N(2)	2.129(5)	2.079(4)
Mn(1)–N(3)	2.110(5)	2.072(4)
C(1)–O(1)	1.173(8)	1.166(6)
C(2)–O(2)	1.167(9)	1.180(6)
Mn(1)–P(1)	2.293(2)	—
Mn(1)–N(7)	—	2.048(4)
N(1)–Mn(1)–N(2)	80.2(2)	84.1(2)
N(1)–Mn(1)–N(3)	82.0(2)	85.3(2)
N(2)–Mn(1)–N(3)	90.3(2)	85.7(2)
C(1)–Mn(1)–C(2)	84.4(4)	86.3(2)
N(2)–Mn(1)–C(2)	174.5(3)	177.9(2)
N(3)–Mn(1)–C(1)	176.2(3)	179.3(2)
N(1)–Mn(1)–P(1)	169.0(2)	—
C(1)–Mn(1)–P(1)	90.0(3)	—
C(2)–Mn(1)–P(1)	93.1(3)	—
N(1)–Mn(1)–N(7)	—	169.3(2)
C(1)–Mn(1)–N(7)	—	93.0(2)
C(2)–Mn(1)–N(7)	—	94.2(2)

Table 4 Crystal and refinement data for $[Mn(CO)_2(PMe_3)\{HC(pz')_3\}][PF_6]$ $\mathbf{2}^+[PF_6]^-$ and $[Mn(CO)_2(py)\{HC(pz')_3\}][PF_6]\cdot 2CH_2Cl_2$ $\mathbf{6}^+[PF_6]^-\cdot 2CH_2Cl_2$

Complex	$\mathbf{2}^+[PF_6]^-$	$\mathbf{6}^+[PF_6]^-\cdot 2CH_2Cl_2$
Formula	$C_{21}H_{31}F_6MnN_6O_2P_2$	$C_{25}H_{31}Cl_4F_6MnN_7O_2P$
Formula weight	630.40	803.28
T/K	173(2)	173(2)
Crystal system	Orthorhombic	Monoclinic
Space group	$P2_12_12_1$	$P2_1/c$
a/Å	12.6906(7)	12.5498(18)
b/Å	12.9537(7)	14.150(2)
c/Å	17.4956(10)	19.981(3)
α (°)	90	90
β (°)	90	100.070(3)
γ (°)	90	90
V/Å^3	2876.1(3)	3493.6(9)
Z	4	4
μ/mm^{-1}	0.639	0.797
Reflections collected	13045	18345
Independent reflections (R_{int})	4118 (0.0489)	6145 (0.0839)
Final $R1$ [$I > 2\sigma(I)$]: R_1, wR_2	0.0642, 0.1493	0.0621, 0.1434

NMR spectroscopy

The ^{1}H NMR spectrum of $\mathbf{1}^+$ shows three equivalent pyrazolyl rings implying C_{3v} symmetry. However, for complexes $\mathbf{2}^+$–$\mathbf{9}^+$ each of the signals for the pyrazolyl protons is split into two, in a 2 : 1 ratio, due to the two rings *trans* to CO and one *trans* to L. The methyl substituents on the pyrazolyl rings also give two signal in the same ratio (see experimental). It was not possible to obtain a well resolved ^{1}H NMR spectrum of $\mathbf{10}^{2+}$ due to its insolubility (in a range of solvents). The $[BPh_4]^-$ salt of $\mathbf{10}^{2+}$ was also insufficiently soluble to provide a useful spectrum.

The ^{31}P NMR spectra of $\mathbf{2}^+$–$\mathbf{5}^+$ were either very broad or did not show a signal for the phosphine/phosphite ligand, probably due to the quadrupolar nature of the manganese centre. Each complex did, however, show a septet at *ca.* −145 ppm for the $[PF_6]^-$ ion.

Table 5 Electrochemical data for $[Mn(CO)_2L\{HC(pz')_3\}]^+$ $\mathbf{1}^+$–$\mathbf{9}^+$ and $[\{HC(pz')_3\}(CO)_2Mn(\mu\text{-}4,4'\text{-bipy})Mn(CO)_2\{HC(pz')_3\}]^{2+}$ $\mathbf{10}^{2+}$ in CH_2Cl_2 at a platinum electrode

Complex	E_p^{ox} (V)[a]
$[Mn(CO)_3\{HC(pz')_3\}]^+$ $\mathbf{1}^+$	1.11
$[Mn(CO)_2(PMe_3)\{HC(pz')_3\}]^+$ $\mathbf{2}^+$	0.38
$[Mn(CO)_2(PEt_3)\{HC(pz')_3\}]^+$ $\mathbf{3}^+$	0.37
$[Mn(CO)_2\{P(OEt_3)\}\{HC(pz')_3\}]^+$ $\mathbf{4}^+$	0.50
$[Mn(CO)_2\{P(OCH_2)_3CEt\}\{HC(pz')_3\}]^+$ $\mathbf{5}^+$	0.69
$[Mn(CO)_2(py)\{HC(pz')_3\}]^+$ $\mathbf{6}^+$	0.13
$[Mn(CO)_2(MeCN)\{HC(pz')_3\}]^+$ $\mathbf{7}^+$	0.21
$[Mn(CO)_2(CNBu^t)\{HC(pz')_3\}]^+$ $\mathbf{8}^+$	0.57
$[Mn(CO)_2(CNXyl)\{HC(pz')_3\}]^+$ $\mathbf{9}^+$	0.68
$[\{HC(pz')_3\}(CO)_2Mn(\mu\text{-}4,4'\text{-bipy})Mn(CO)_2\{HC(pz')_3\}]^{2+}$ $\mathbf{10}^{2+}$	0.68

[a] Potentials are calibrated *vs.* $[Fe(\eta^5\text{-}C_5H_5)_2]$ (at 0.00 V) or $[Fe(\eta^5\text{-}C_5Me_5)_2]$ (at −0.55 V).

IR spectroscopy

The IR spectrum of $\mathbf{1}^+[PF_6]^-$ shows two carbonyl stretching absorptions, at 2045 and 1950 cm^{-1}. The lower energy band is broad, consistent with a tricarbonyl complex with C_{3v} symmetry. These absorptions are very similar in energy to those reported for the analogous triflate salt, at 2044 and 1949 cm^{-1},[8] and the rhenium complex $[Re(CO)_3\{HC(pz')_3\}]Br$, at 2036 and 1930 cm^{-1}.[22] Complexes $\mathbf{2}^+$–$\mathbf{9}^+$ and $\mathbf{10}^{2+}$ each show two strong IR carbonyl bands consistent with C_{2v} symmetry. These vary in energy by 46 cm^{-1} depending on the electron-donating/accepting ability of the co-ligand. Complexes $\mathbf{8}^+$ and $\mathbf{9}^+$ also show a CN stretch due to the isocyanide ligands (Table 1). Frequencies for the complexes $\mathbf{2}^+$–$\mathbf{9}^+$ increase in the order L = PEt_3 < py < PMe_3 < MeCN < $P(OEt)_3$ < *t*BuNC < XylNC < $P(OCH_2)_3CEt$, consistent with accepted trends in electron donor and acceptor ability for these ligands.[23–25]

The relative electron-donating ability of the ligands Tp′, Tp, Cp* and Cp varies with metal, oxidation state and co-ligands.[26,27] For Group 7 carbonyl complexes there is some ambiguity as to the trends in electron donating ability of Cp and Tp type ligands.[26] However, for manganese, in general the Cp ligands are more electron donating than the Tp ligands. The carbonyl stretching frequency for the pyrazolylmethane complex is greater than that observed for the pyrazolylborate and cyclopentadienyl complexes (Table 2). However, the complexes of Cp*, Cp, Tp′ and Tp are neutral whereas $\mathbf{1}^+$ is cationic. The positive charge on the metal reduces back donation to the CO ligands thus, increasing

ν(CO). Overall, the electron-donating ability of the ligands for manganese(I) complexes follows the trend:

$$Cp^* > Cp \approx Tp' > Tp > HC(pz')_3$$

Solid state structural analysis

The structures of $[Mn(CO)_2(PMe_3)\{HC(pz')_3\}]^+$ $\mathbf{2}^+$ and $[Mn(CO)_2(py)\{HC(pz')_3\}]^+$ $\mathbf{6}^+$ as $[PF_6]^-$ salts were determined by X-ray crystallography (Tables 3 and 4). Crystals of each were grown by allowing *n*-hexane to diffuse slowly into a concentrated CH_2Cl_2 solution of the complex at –20 °C.

The structure of $\mathbf{2}^+$ is distorted octahedral (Fig. 3) with N(1)–Mn–N(2), N(2)–Mn–N(3) and N(1)–Mn–N(3) angles of 80.2(2), 90.3(2) and 82.0(2)° respectively. The tridentate tris(3,5-dimethylpyrazolyl)methane ligand facially caps three co-ordination sites of the octahedral manganese. The pyrazolyl ring *trans* to the phosphine is closer to the metal centre than the pyrazolyl rings *trans* to carbonyls, with an Mn–N(1) bond length of 2.064(5) Å compared to 2.129(5) and 2.110(5) Å for Mn–N(2) and Mn–N(3).

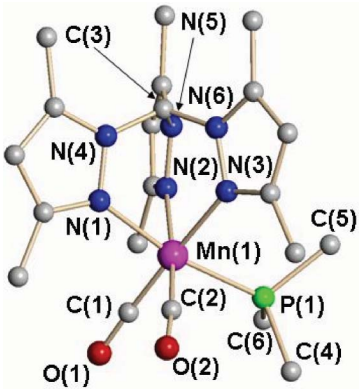

Fig. 3 The structure of $[Mn(CO)_2(PMe_3)\{HC(pz')_3\}]^+$ $\mathbf{2}^+$. The hydrogen atoms have been omitted for clarity.

The related pyrazolylborate complex $[Mn(CO)_2\{P(OMe)_3\}Tp']$ crystallises with two independent molecules in the unit cell and has N(1)–Mn–N(2), N(2)–Mn–N(3) and N(1)–Mn–N(3) angles of 84.1(1), 85.3(1) and 93.5(1)° and 84.3(1), 83.0(1) and 90.9(1)° respectively.[29] In one of the molecules, the pyrazolyl ring *trans* to the phosphite is closer to the metal centre than the pyrazolyl rings *trans* to carbonyls with an Mn–N(1) bond length of 2.046(2) Å compared to 2.143(3) and 2.104(3) Å for Mn–N(2) and Mn–N(3). However, in the second molecule, the bond length for Mn–N(1) {2.106(2) Å} lies between the bond lengths for Mn–N(2) and Mn–N(3) {2.078(3) and 2.161(3) Å}.

The structure of $\mathbf{6}^+$ shows the same general features as that of $\mathbf{2}^+$ in that it is also distorted octahedral (Fig. 4) with a facially capping tris(3,5-dimethylpyrazolyl)methane ligand. Again, the pyrazolyl ring *trans* to pyridine is closer to the metal centre than the pyrazolyl rings *trans* to carbonyls, with an Mn–N(1) bond length of 2.052(4) Å compared to Mn–N(2) and Mn–N(3) bond lengths of 2.079(4) and 2.072(4) Å respectively. In addition, the $Mn–N_{(pyrazolyl)}$ bond lengths for $\mathbf{6}^+$ {2.052(4), 2.079(4) and 2.072(4) Å} are slightly shorter (and more similar) than for $\mathbf{2}^+$ {2.064(5), 2.129(5) and 2.110(5) Å}.

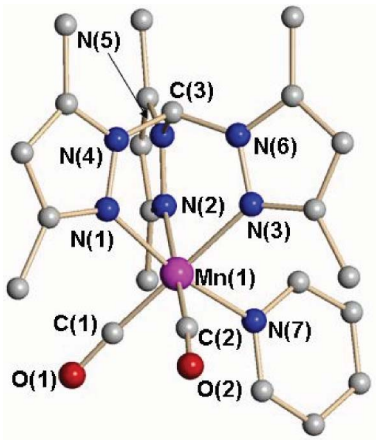

Fig. 4 The structure of $[Mn(CO)_2(py)\{HC(pz')_3\}]^+$ $\mathbf{6}^+$. The hydrogen atoms, have been omitted for clarity.

Electrochemical studies

The cyclic voltammograms in CH_2Cl_2 of the complexes $[Mn(CO)_2L\{HC(pz')_3\}]^+$ {L = CO $\mathbf{1}^+$, PMe_3 $\mathbf{2}^+$, PEt_3 $\mathbf{3}^+$, $P(OEt)_3$ $\mathbf{4}^+$, $P(OCH_2)_3CEt$ $\mathbf{5}^+$, py $\mathbf{6}^+$, MeCN $\mathbf{7}^+$, CN*t*Bu $\mathbf{8}^+$, CNXyl $\mathbf{9}^+$ and $[\{HC(pz')_3\}(CO)_2Mn(\mu\text{-}4,4\text{-bipy})Mn(CO)_2\{HC(pz')_3\}]^{2+}$ $\mathbf{10}^{2+}$ each show an irreversible oxidation wave in the potential range 0.13 to 1.11 V (Table 5). Complex $\mathbf{10}^{2+}$ also shows a partially reversible reduction at –1.35 V $\{I_{(red)}/I_{(ox)} = 0.84$ at a scan rate of 200 mV $s^{-1}\}$ (Fig. 5). Given that all of the complexes $\mathbf{2}^+$–$\mathbf{9}^+$ are yellow or orange, the purple colour of $\mathbf{10}^{2+}$ suggests electron-transfer processes which must differ from those of the mononuclear complexes. Intervalence charge transfer should result in two oxidation waves in the cyclic voltammogram where only one is observed. However, given an irreversible oxidation, it is possible that decomposition occurs before a second oxidation is observed.

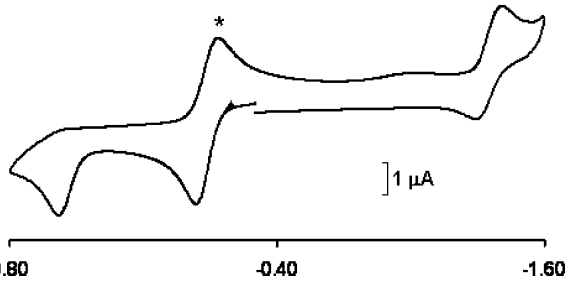

Fig. 5 Cyclic voltammogram of $[\{HC(pz')_3\}Mn(CO)_2(4,4'\text{-bipy})\text{-}Mn(CO)_2\{HC(pz')_3\}]^{2+}$ $\mathbf{10}^{2+}$ in CH_2Cl_2 at a platinum electrode (* = oxidation wave of $[FeCp_2]$ calibrated to 0.0 V).

As reflected in the IR spectra with decreasing ν(CO) for stronger donors, the increase in electron density at the metal results in lower oxidation potentials (*i.e.* there is a direct between the carbonyl stretching frequencies and the oxidation potential). A plot of $E^{0\prime}$ against the average carbonyl stretching frequency for $[Mn(CO)_2L(\eta^5\text{-}C_5H_{5-n}Me_n)]$ is linear.[15] As the oxidations of $\mathbf{1}^+$–$\mathbf{10}^{2+}$ are irreversible, E^0 values were estimated from the peak potentials (assuming fully reversible systems and approximated by comparison with the peak to peak separation of the ferrocene calibrant). The plot of $\nu(CO)_{ave}$ against the estimated E^0 values for

the tris(3,5-dimethylpyrazolyl)methane complexes described here is also linear and coincident with that for the cyclopentadienyl series (R^2 = 0.99) (Fig. 6). However, the data points for the acetonitrile complexes $[Mn(CO)_2(NCMe)\{HC(pz')_3\}]^+$ **7**$^+$ (shown in pink) and $[Mn(CO)_2(NCMe)(\eta^5\text{-}C_5H_4Me)]$ (green), the pyridine complex $[Mn(CO)_2(py)\{HC(pz')_3\}]^+$ **6**$^+$ (orange) and bimetallic $[\{HC(pz')_3\}(CO)_2Mn(\mu\text{-}4,4'\text{-bipy})Mn(CO)_2\{HC(pz')_3\}]^{2+}$ **10**$^{2+}$ (purple) do not lie on the same line. DFT studies reveal subtle differences in the HOMO which explain the different behaviour of the complexes of *N*- and *P*-donors (see below).

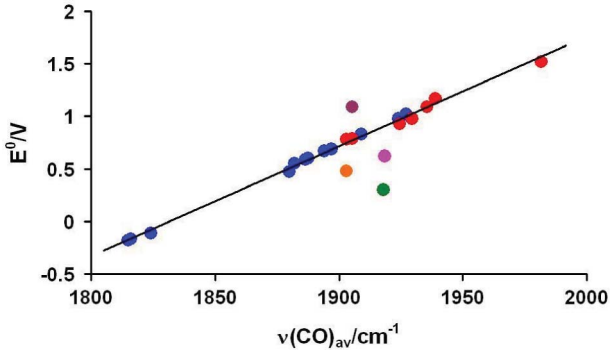

Fig. 6 A plot of $E^{0\prime}$ against $\nu(CO)_{ave}$ for $[Mn(CO)_{3-m}L_m(\eta^5\text{-}C_5H_{5-n}Me_n)]$ (n = 0, 1 or 5; m = 1 or 2) (blue) and $[Mn(CO)_2L\{HC(pz')_3\}][PF_6]$ (red).

Density Functional Theory calculations

In an attempt to elucidate further the nature of the bonding within this series of complexes, density functional theory (DFT) calculations (computed using the B3PW91 hybrid functional) were undertaken on the phosphine complex **2**$^+$, the pyridine complex **6**$^+$ and the 4,4′-bipyridine bridged complex **10**$^{2+}$.

Firstly, the predicted lowest energy conformations of **2**$^+$ and **6**$^+$ are similar to that observed experimentally. In both complexes, the pyrazolyl ring *trans* to L is closer to Mn {2.057 Å for **2**$^+$; 2.045 for **6**$^+$ Å} than the pyrazolyl rings *trans* to carbonyls (2.153 and 2.126 Å for **2**$^+$; 2.089 and 2.089 Å for **6**$^+$). In addition, the Mn–$N_{(pyrazolyl)}$ bond lengths for **6**$^+$ are shorter (and more similar) than for **2**$^+$ as seen experimentally.

Although absolute values for stretching frequencies within the complexes cannot be reliably determined, relative values can be obtained. In order to determine the reasons for complexes of *N*-donor ligands not conforming to the expected trend, theoretical carbonyl stretching frequencies were determined for each complex. The average calculated value for **2**$^+$ (1981 and 2038 cm^{-1}) is 8 cm^{-1} lower than that for **6**$^+$ (1989 and 2045 cm^{-1}). However, this is not in accord with the experimental values in which the average CO stretching frequency of **2**$^+$ is 3 cm^{-1} *higher* than that of **6**$^+$.

An analysis of the frontier orbitals provides a qualitative insight into the bonding characteristics of each complex (Fig. 7). For the pyridine complex, **6**$^+$, the HOMO (E = −7.86 eV) is mainly a π orbital between the metal and the CO ligands (backbonding). There is also orbital coverage on the pyridine ligand. However, there is a node (and resultant phase change) between the metal and the *N*-donor. Therefore, the HOMO does not contain any M–N bonding character. For the phosphine complex, **2**$^+$, the HOMO (E = −8.11 eV) is again mostly a π orbital situated on manganese

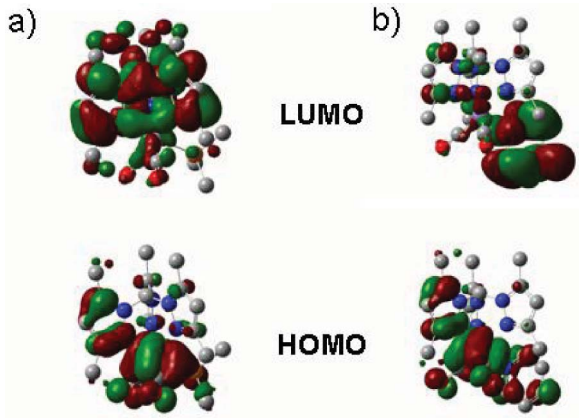

Fig. 7 The frontier orbitals of a) **2**$^+$ and b) **6**$^+$.

and the CO ligands. However, the HOMO also located over the M–P bond with no node (or phase change). The contiguous nature of the HOMO results in an association between the M–CO and M–P bonds. These intimately entwined molecular orbitals could explain the correlation between CO stretching energies and the oxidation potentials of the complexes of phosphine ligands. The node (and resultant phase change) between the metal and *N*-donor ligands results in a different relationship with the CO ligands and, therefore, offers a possible explanation for why the plot of average CO stretching frequency *vs*. oxidation potential does not lie on the line of phosphine complexes.

It is noteworthy that for **2**$^+$, two of the lowest unoccupied orbitals are sufficiently close in energy to be considered isoenergetic (ΔE <0.2 eV). The LUMO (E = −3.78 eV) {and LUMO+1 (E = −3.65 eV)} are situated primarily on the tris(3,5-dimethylpyrazolyl)methane ligand. By contrast, for **6**$^+$ the LUMO (E = −4.00 eV) is situated primarily on the pyridine ligand. The frontier orbitals of **10**$^{2+}$ are similar in location to the pyridine complex **6**$^+$ (Fig. 8). The HOMO (–9.14 eV) and HOMO-1

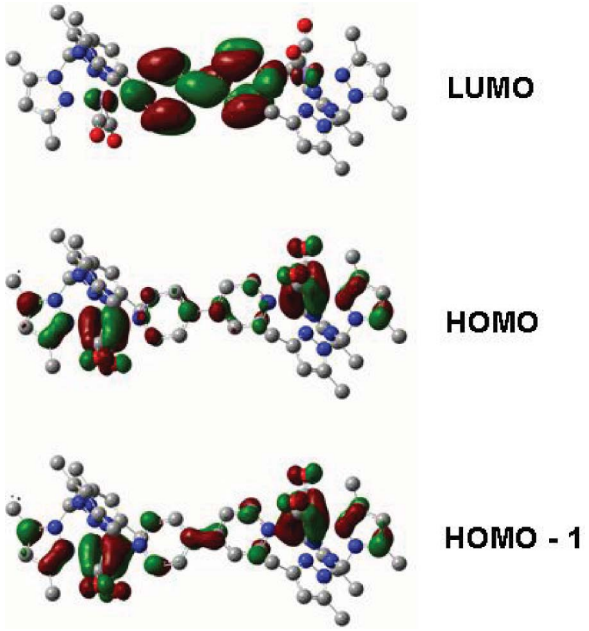

Fig. 8 Graphical representation of the frontier orbitals for **10**$^{2+}$.

(–9.31 eV) can be considered isoenergetic and are lower than for $\mathbf{6}^+$. This results in greater stabilisation of the complex and an increase in oxidation potential, as seen experimentally. Both orbitals are situated on the manganese metal centres and CO ligands with some electron density on the 4-position of the 4,4′-bipyridine ligand. There is again a node (and phase change) between the metal and the *N*-donor ligands as observed in the monometallic complex. The LUMO is situated almost entirely on the 4,4′-bipyridine ligand. The location of the frontier orbitals (and the purple colour of the complex) suggest that an MLCT transition is occurring. The HOMO–LUMO bandgap for $\mathbf{10}^{2+}$ ($E_{bandgap}$ = 2.67 eV) is much smaller than for $\mathbf{2}^+$ ($E_{bandgap}$ = 4.33 eV) or $\mathbf{6}^+$ ($E_{bandgap}$ = 3.86 eV). This results in the lowest energy absorption (464 nm *cf*. 287 and 321 nm for $\mathbf{2}^+$ and $\mathbf{6}^+$ respectively) falling into the visible region giving a possible explanation for the observed colour. Interestingly, rotation about the 4,4′-position of the bipyridine ligand of 28° from planarity gives the lowest energy configuration.

Conclusions

The first examples of manganese dicarbonyl complexes bearing a neutral pyrazolylmethane ligand, **[Mn(CO)$_2$L{HC(pz′)$_3$}][PF$_6$]**, were prepared from the parent tricarbonyl using Me_3NO in the presence of co-ordinating lignds. X-ray crystallography has shown that similar structures are adopted for complexes with *P*- and *N*-donor ligands. Pyrazolyl rings *trans* to these ligands are closer to the metal than those *trans* to carbonyls. Pyrazolyl rings are slightly closer to the metal (and more similar) for the pyridine complex compared to the phosphine complex.

There is a direct correlation between the average carbonyl stretching frequency and the oxidation potential for complexes of *P*-donor ligands. A plot of $\nu(CO)_{ave}$ *vs*. $E^{0\prime}$ is linear and coincident with the correlation observed for $[Mn(CO)_{3-m}L_m(\eta\text{-}C_5H_{5-n}Me_n)]$. The data for *N*-donor ligands do not lie on this line. A possible explanation is offered by DFT analysis of $\mathbf{2}^+$, $\mathbf{6}^+$ and $\mathbf{10}^{2+}$ which shows the contiguous HOMO located over the M–CO and the M–P bonds for the *P*-donor whereas a node exists between the metal and *N*-donors.

Reaction of $[Mn(CO)_2(NCMe)\{HC(pz')_3\}]^+$ with half an equivalent of 4,4′-bipyridine, yields a purple compound assumed to be $[\{HC(pz')_3\}(CO)_2Mn(\mu\text{-}4,4'\text{-bipy})Mn(CO)_2\{HC(pz')_3\}]^{2+}$. The smaller HOMO–LUMO bandgap compared with the mononuclear complexes results in lower energy absorptions and a possible explanation for the colour of the complex, as determined by DFT studies.

Experimental

The preparation, purification and reactions of the complexes described were carried out using Schlenk techniques under an atmosphere of dry nitrogen using solvents dried by Anhydrous Engineering double alumina or alumina/copper catalyst columns. All solvents were deoxygenated prior to use unless otherwise stated. The compounds $[MnBr(CO)_5]$[30] and $HC(pz')_3$[8,31] were prepared by published methods.

X-Ray diffraction studies were performed on a Siemens three-circle SMART area diffractometer. All calculations were made with programmes of the SHELXTL system.[32]

DFT studies were performed using the Gaussian 03 suite of programs.[33] Calculations were carried out with the hybrid B3PW91 functional, with the 6-31G(d,p) basis set for manganese and the coordinating atoms and 6-31G basis set for all other atoms. Geometry optimisations were performed without restraints, followed by frequency calculations to ascertain the nature of the resulting structure (minimum *vs*. transition state).

NMR spectra were recorded on a JEOL GX270 or JEOL λ300 spectrometer with $SiMe_4$ as an internal standard. ^{31}P NMR spectra were recorded at 121 MHz.

Electrochemical studies were carried out using an EG&G model 273A potentiostat linked to a computer using EG&G Model 270 Research Electrochemistry software in conjunction with a three-electrode cell. The auxiliary electrode was a platinum wire and the working electrode a platinum disc (1.6 mm diameter). The reference was an aqueous saturated calomel electrode separated from the test solution by a fine porosity frit and an agar bridge saturated with KCl. Solutions were 1.0×10^{-3} mol dm^{-3} in the test compound and 0.1 mol dm^{-3} in $[NnBu_4][PF_6]$ as the supporting electrolyte. The solvent used was CH_2Cl_2. Data are calibrated using $[Fe(\eta^5\text{-}C_5H_5)_2]$ or $[Fe(\eta^5\text{-}C_5Me_5)_2]$ added to the test solutions as an internal calibrant. Under these conditions, $E^{0\prime}$ for the one-electron oxidation of $[Fe(\eta\text{-}C_5H_5)_2]$ and $[Fe(\eta^5\text{-}C_5Me_5)_2]$ is set to 0.00 and –0.55 V respectively. Unless specified, all electrochemical values are at a scan rate of 200 mVs^{-1}.

Microanalyses were carried out by the staff of the Microanalytical Service of the School of Chemistry, University of Bristol.

Synthesis

[Mn(CO)$_3${HC(pz′)$_3$}][PF$_6$] 1$^+$[PF$_6$]$^-$. A solution of $[MnBr(CO)_5]$ (1.36 g, 4.96 mmol) and $HC(pz')_3$ (1.509 g, 5.06 mmol) in toluene (75 cm^3) was heated under reflux for 2 h during which time a yellow precipitate was formed. The mixture was allowed to reach room temperature and the pale yellow mother liquors decanted. The yellow powder was dissolved in water (60 cm^3) and then $[NH_4][PF_6]$ (825 mg, 5.06 mmol) was added to precipitate a pale yellow solid. The mixture was stirred for 1 h and the precipitate collected. The yellow powder was washed with water (2 × 30 cm^3) and then dried *in vacuo*, yield 2.31 g (80%). ^{1}H NMR (270 MHz, CD_2Cl_2) δ_H = 7.79 {1H, s, *H*C(pz′)$_3$}, 6.18 (3H, s, PzC*H*), 2.59 (9H, s, PzC*H*$_3$), 2.58 (9H, s, PzC*H*$_3$) ppm.

General procedure for the synthesis of [Mn(CO)$_2$L{HC(pz′)$_3$}][PF$_6$] 3$^+$–6$^+$ and 8$^+$–9$^+$. Solid Me_3NO (18 mg, 0.240 mmol) was added to a solution of $[Mn(CO)_3\{HC(pz')_3\}][PF_6]$ (140 mg, 0.240 mmol) and L (1 equiv.) in CH_2Cl_2 (20 cm^3) and the mixture stirred for 10 min. Small portions of Me_3NO (*ca.* 1 mg) were added until the reaction was complete (shown by IR spectroscopy). The resulting yellow or orange solution was filtered and then concentrated *in vacuo*. *n*-Hexane was then added to precipitate a powder, which was washed with *n*-hexane (2 × 20 cm^3) and dried *in vacuo*.

[Mn(CO)$_2$(PEt$_3$){HC(pz′)$_3$}][PF$_6$] 3$^+$[PF$_6$]$^-$. Yield 144 mg (89%). ^{1}H NMR (270 MHz, CD_2Cl_2) δ_H = 7.66 {1H, s, *H*C(pz′)$_3$}, 6.24 (2H, s, PzC*H*), 5.89 (1H, s, PzC*H*), 2.67 (6H, s, PzC*H*$_3$), 2.63 (6H, s, PzC*H*$_3$), 2.53 (3H, s, PzC*H*$_3$), 2.39 (3H, s, PzC*H*$_3$),

1.60–1.75 {6H, dq, $J_{H,P}$ = 7 Hz, $J_{H,H}$ = 7 Hz, P(CH_2CH$_3$)$_3$}, 0.69–0.87 {9H, dt, $J_{H,P}$ = 7 Hz, $J_{H,H}$ = 7 Hz, P(CH$_2$CH_3)$_3$} ppm.

[Mn(CO)$_2${P(OEt)$_3$}{HC(pz′)$_3$}][PF$_6$] 4$^+$[PF$_6$]$^-$. Yield 166 mg (96%). ^{1}H NMR (270 MHz, CD_2Cl_2) δ_H = 7.72 {1H, s, HC(pz′)$_3$}, 6.18 (2H, s, PzCH), 5.98 (1H, s, PzCH), 3.71 {6H, dq, $J_{H,P}$ = 7 Hz, $J_{H,H}$ = 7 Hz, P(OCH_2CH$_3$)$_3$}, 2.66 (6H, s, PzCH_3), 2.61 (6H, s, PzCH_3), 2.54 (3H, s, PzCH_3), 2.45 (3H, s, PzCH_3), 1.19 {9H, t, $J_{H,H}$ = 7 Hz, P(OCH$_2$CH_3)$_3$} ppm.

[Mn(CO)$_2${P(OCH$_2$)$_3$CEt}{HC(pz′)$_3$}][PF$_6$] 5$^+$[PF$_6$]$^-$. Yield 141 mg (82%). ^{1}H NMR (270 MHz, CD_2Cl_2) δ_H = 7.60 {1H, s, HC(pz′)$_3$}, 6.08 (2H, s, PzCH), 5.95 (1H, s, PzCH), 4.14 {6H, br s, P(OCH_2)$_3$CEt}, 2.00–2.85 (18H, br m, PzCH_3), 1.15 {2H, s, P(OCH$_2$)$_3$CCH_2CH$_3$}, 0.74 {3H, s, P(OCH$_2$)$_3$CCH$_2$CH_3} ppm.

[Mn(CO)$_2$(py){HC(pz′)$_3$}][PF$_6$] 6$^+$[PF$_6$]$^-$. Yield 143 mg (94%). ^{1}H NMR (270 MHz, CD_2Cl_2) δ_H = 8.85 (1H, br s, pyCH), 7.95 {1H, s, HC(pz′)$_3$}, 7.62 (1H, br s, pyCH), 7.33 (1H, br s, pyCH), 7.14 (1H, br s, pyCH), 7.00 (1H, br s, pyCH), 6.20 (2H, s, PzCH), 5.89 (1H, s, PzCH), 2.69 (6H, s, PzCH_3), 2.50 (3H, s, PzCH_3), 2.45 (3H, s, PzCH_3), 1.80 (6H, s, PzCH_3) ppm.

[Mn(CO)$_2$(CNBu^t){HC(pz′)$_3$}][PF$_6$] 8$^+$[PF$_6$]$^-$. Yield 130 mg (85%). ^{1}H NMR (270 MHz, CD_2Cl_2) δ_H = 7.72 {1H, s, HC(pz′)$_3$}, 6.14 (2H, s, PzCH), 6.04 (1H, s, PzCH), 2.45–2.65 (18H, br m, PzCH_3), 1.48 {9H, s, (CH_3)$_3$CNC} ppm.

[Mn(CO)$_2$(CNXyl){HC(pz′)$_3$}][PF$_6$] 9$^+$[PF$_6$]$^-$. Yield 140 mg (85%). ^{1}H NMR (270 MHz, CD_2Cl_2) δ_H = 7.79 {1H, s, HC(pz′)$_3$}, 7.14 (3H, br s, 2,6-Me$_2$C$_6$$H_3$NC), 6.15 (2H, s, PzC$H$), 6.09 (1H, s, PzC$H$), 2.60 (9H, br s, PzC$H_3$), 2.55 (9H, br s, PzC$H_3$), 2.33 {6H, s, 2,6-(C$H_3$)$_2C_6H_3$NC} ppm.

[Mn(CO)$_2$(NCMe){HC(pz′)$_3$}][PF$_6$] 7$^+$[PF$_6$]$^-$. Solid Me$_3$NO (38 mg, 0.506 mmol) was added to a solution of [Mn(CO)$_3${HC(pz′)$_3$}][PF$_6$] (300 mg, 0.515 mmol) in MeCN and the mixture stirred for 15 min. Small aliquots of Me$_3$NO (*ca.* 1 mg) were added until the reaction was complete. The solvent was removed *in vacuo* and the crude product dissolved in CH_2Cl_2 (10 ml). The orange solution was filtered through Celite and concentrated *in vacuo* before *n*-hexane was added to precipitate an orange powder which was washed with *n*-hexane (2 × 20 cm^3) and dried *in vacuo*, yield 279 mg (91%). ^{1}H NMR (270 MHz, CD_2Cl_2) δ_H = 7.82 {1H, s, HC(pz′)$_3$}, 6.22 (2H, s, PzCH), 5.89 (1H, s, PzCH), 2.62 (6H, s, PzCH_3), 2.56 (6H, s, PzCH_3), 2.47 (3H, s, PzCH_3), 2.39 (3H, s, PzCH_3), 2.17 (3H, s, CH_3CN) ppm.

[Mn(CO)$_2$(PMe$_3$){HC(pz′)$_3$}][PF$_6$] 2$^+$[PF$_6$]$^-$. A solution of [Mn(CO)$_2$(NCMe){HC(pz′)$_3$}][PF$_6$] (115 mg, 0.193 mmol) and PMe$_3$ (30 µl, 0.289 mmol) in CH_2Cl_2 (20 cm^3) was stirred for 30 min, then filtered and concentrated *in vacuo*. *n*-Hexane was added to precipitate a yellow solid which was washed with *n*-hexane (2 × 20 cm^3) and dried *in* vacuo, yield 116 mg (95%). ^{1}H NMR (270 MHz, CD_2Cl_2) δ_H = 7.58 {1H, s, HC(pz′)$_3$}, 6.14 (2H, s, PzCH), 5.82 (1H, s, PzCH), 2.58 (6H, s, PzCH_3), 2.54 (6H, s, PzCH_3), 2.43 (3H, s, PzCH_3), 2.32 (3H, s, PzCH_3), 1.23 {9H, d, $J_{H,P}$ = 8 Hz, P(CH_3)$_3$} ppm.

[{HC(pz′)$_3$}(CO)$_2$Mn(µ-4,4′-bipy)Mn(CO)$_2${HC(pz′)$_3$}][PF$_6$]$_2$ 10^{2+} 2[PF$_6$]$^-$. A solution of [Mn(CO)$_2$(NCMe){HC(pz′)$_3$}][PF$_6$] (126 mg, 0.212 mmol) and 4,4′-bipyridine (17 mg, 0.109 mmol) in CH_2Cl_2 (20 cm^3) was stirred for 45 min, then filtered and concentrated *in vacuo*. *n*-Hexane was added to precipitate a purple solid which was washed with *n*-hexane (2 × 20 cm^3) and dried *in* vacuo, yield 110 mg (82%).

Acknowledgements

We thank the EPSRC (R.A.B) and the School of Chemistry, University of Bristol (A.J.H.) for Postgraduate Scholarships. Prof. N. G. Connelly (University of Bristol) is also gratefully acknowledged.

Notes and references

1 H. R. Bigmore, S. C. Lawrence, P. Mountford and C. S. Tredget, *Dalton Trans.*, 2005, 635.
2 M. G. Cushion and P. Mountford, *Chem. Commun.*, 2011, **47**, 2276.
3 S. Trofimenko, *Chem. Rev.*, 1993, **93**, 943.
4 S. Trofimenko, *Scorpionates: The Co-ordination Chemistry of Polypyrazolylborate Ligands*Imperial College Press: London, 1999.
5 C. Pettinari and C. Santini, Polypyrazolylborate and Scorpionate Ligands; In J. A. McClevery and T. H. Meyer, ed., *Comprehensive Co-ordination Chemistry II -From Biology to Nanotechnology*Elsevier Ltd: Oxford, U. K, 2004; Vol. 1, pp 159–210.
6 C. Pettinari and R. Pettinari, *Coord. Chem. Rev.*, 2005, **249**, 525 and references therein.
7 A. F. R. Kilpatrick, S. V. Kulangara, M. G. Cushion, R. Duchateau and P. Mountford, *Dalton Trans.*, 2010, **39**, 3653.
8 D. L. Reger, T. C. Grattan, K. J. Brown, C. A. Little, J. J. S. Lamba, A. L. Rheingold and R. D. Sommer, *J. Organomet. Chem.*, 2000, **607**, 120.
9 Z. Pang, T. J. Burkey and R. F. Johnson, *Organometallics*, 1997, **16**, 120.
10 P. C. Kunz, W. Huber, A. Rojas, U. Schatzschneider and B. Spingler, *Eur. J. Inorg. Chem.*, 2009, 5358.
11 J. Niesel, A. Pinto, H. W. Peindy N'Dongo, K. Merz, I. Ott, R. Gust and U. Schatzschneider, *Chem. Commun.*, 2008, 1798.
12 H. Pfeiffer, A. Rojas, J. Niesel and U. Schatzschneider, *Dalton Trans.*, 2009, 4292.
13 D. L. Reger, R. F. Semeniuc and M. D. Smith, *J. Organomet. Chem.*, 2003, **666**, 87.
14 A. R. Schoenberg and W. P. Anderson, *Inorg. Chem.*, 1974, **13**, 465.
15 N. G. Connelly and M. D. Kitchen, *J. Chem. Soc., Dalton Trans.*, 1977, 931.
16 O. Kaufhold, A. Stasch, P. G. Edwards and F. E. Hahn, *Chem. Commun.*, 2007, 1822.
17 O. Kaufhold, A. Stasch, T. Pape, A. Hepp, P. G. Edwards, P. D. Newman and F. E. Hahn, *J. Am. Chem. Soc.*, 2009, **131**, 307.
18 S. Trofimenko, *J. Am. Chem. Soc.*, 1970, **92**, 5118.
19 D. L. Reger, R. F. Semeniuc and M. D. Smith, *J. Chem. Soc., Dalton Trans.*, 2002, 476.
20 D. L. Reger, J. R. Gardinier, T. C. Grattan and M. D. Smith, *J. Organomet. Chem.*, 2005, **690**, 1901.
21 A. R. Schoenberg and W. P. Anderson, *Inorg. Chem.*, 1972, **11**, 85.
22 D. L. Reger, K. J. Brown and M. D. Smith, *J. Organomet. Chem.*, 2002, **658**, 50.
23 C. A. Streuli, *Anal. Chem.*, 1960, **32**, 985.
24 E. M. Thorsteinson and F. Basolo, *J. Am. Chem. Soc.*, 1966, **88**, 3929.
25 W. A. G. Graham, *Inorg. Chem.*, 1968, **7**, 315.
26 D. M. Tellers, S. J. Skoog, R. G. Bergman, T. B. Gunnoe and W. D. Harman, *Organometallics*, 2000, **19**, 2428 and references therein.
27 K. Fujisawa, T. Ono, Y. Ishikawa, N. Amir, Y. Miyashita, K. Okamoto and N. Lehnert, *Inorg. Chem.*, 2006, **45**, 1698.
28 R. B. King and A. J. Efraty, *J. Am. Chem. Soc.*, 1972, **94**, 3773.
29 J. E. Joachim, C. Apostolidis, B. Kanellakopulos, D. Meyer, B. Nuber, K. Raptis, J. Rebizant and M. L. Ziegler, *J. Organomet. Chem.*, 1995, **492**, 199.
30 E. W. Abel and G. Wilkinson, *J. Chem. Soc.*, 1959, 1501.
31 A. J. Hallett, K. M. Anderson, N. G. Connelly and M. F. Haddow, *Dalton Trans.*, 2009, 4181.
32 *SHELXTS-PC Package*, Bruker Analytical X-ray Systems, Madison WI, 1998.
33 M. J. Frisch, G. W. Trucks, H. B. Schlegel, G. E. Scuseria, M. A. Robb, J. R. Cheeseman, J. A. Montgomery, Jr., T. Vreven, K. N.

Kudin, J. C. Burant, J. M. Millam, S. S. Iyengar, J. Tomasi, V. Barone, B. Mennucci, M. Cossi, G. Scalmani, N. Rega, G. A. Petersson, H. Nakatsuji, M. Hada, M. Ehara, K. Toyota, R. Fukuda, J. Hasegawa, M. Ishida, T. Nakajima, Y. Honda, O. Kitao, H. Nakai, M. Klene, X. Li, J. E. Knox, H. P. Hratchian, J. B. Cross, V. Bakken, C. Adamo, J. Jaramillo, R. Gomperts, R. E. Stratmann, O. Yazyev, A. J. Austin, R. Cammi, C. Pomelli, J. Ochterski, P. Y. Ayala, K. Morokuma, G. A. Voth, P. Salvador, J. J. Dannenberg, V. G. Zakrzewski, S. Dapprich, A. D. Daniels, M. C. Strain, O. Farkas, D. K. Malick, A. D. Rabuck, K. Raghavachari, J. B. Foresman, J. V. Ortiz, Q. Cui, A. G. Baboul, S. Clifford, J. Cioslowski, B. B. Stefanov, G. Liu, A. Liashenko, P. Piskorz, I. Komaromi, R. L. Martin, D. J. Fox, T. Keith, M. A. Al-Laham, C. Y. Peng, A. Nanayakkara, M. Challacombe, P. M. W. Gill, B. G. Johnson, W. Chen, M. W. Wong, C. Gonzalez and J. A. Pople, *GAUSSIAN 03 (Revision B.03)*, Gaussian, Inc., Wallingford, CT, 2004.